# Phase-shifter using submicron silicon waveguide couplers with ultra-small electro-mechanical actuator



doi: 10.1364/OE.18.007031

# Phase-shifter using submicron silicon waveguide couplers with ultra-small electro-mechanical actuator

**Taro Ikeda,[1] Kazunori Takahashi,[1] Yoshiaki Kanamori,[1] and Kazuhiro Hane[1],***

[1]*Department of Nanomechanics, Tohoku University, Sendai 980-8579, Japan*
**hane2@hane .mech.tohoku.ac.jp*

**Abstract:** Phase shifter is an important part of optical waveguide circuits as used in interferometer. However, it is not always easy to generate a large phase shift in a small region. Here, a variable phase-shifter operating as delay-line of silicon waveguide was designed and fabricated by silicon micromachining. The proposed phase-shifter consists of a freestanding submicron-wide silicon waveguide with two waveguide couplers and an ultrasmall silicon comb-drive actuator. The position of the freestanding waveguide is moved by the actuator to vary the total optical path. Phase-shift was measured in a Mach-Zehnder interferometer to be 3.0π at the displacement of 1.0 μm at the voltage of 31V. The dimension of the fabricated device is 50μm wide and 85μm long.



**OCIS codes:** (230.4685) Optical microelectromechanical devices; (060.1810) Couplers; (250.5300) Photonic integrated circuits.

## References and links

1. B. Jalali, and S. Fathpour, "Silicon photonics," J. Lightwave Technol. **24**(12), 4600–4615 (2006).
2. H. Yamada, T. Chu, S. Ishida, and Y. Arakawa, "Si photonic wire waveguide devices," IEEE J. Sel. Top. Quantum Electron. **12**(6), 1371–1379 (2006).
3. A. Sasaki, G. Hara, and T. Baba, "Propagation characteristics of ultrahigh-Δ optical waveguide on silicon-on-insulator substrate," Jpn. J. Appl. Phys. **40**(Part 2, No. 4B), L383–L385 (2001).
4. W. Bogaerts, P. Dumon, D. V. Thourhout, D. Taillaert, P. Jaenen, J. Wouters, S. Beckx, V. Wiaux, and R. G. Baets, "Compact wavelength-selective functions in silicon-on-insulator photonics wires," IEEE J. Sel. Top. Quantum Electron. **12**(6), 1394–1401 (2006).
5. K. Sasaki, F. Ohno, A. Motegi, and T. Baba, "Arrayed waveguide grating of 70x60μm$^2$ size based on Si photonic wire waveguides," Electron. Lett. **41**(14), 801–802 (2005).
6. A. Vorckel, M. Monster, W. Henschel, P. H. Bolivar, and H. Kurz, "Asymmetrically coupled silicon-on-insulator microring resonators for compact add-drop multiplexers," IEEE Photon. Technol. Lett. **15**(7), 921–923 (2003).
7. K. Takahashi, Y. Kanamori, Y. Kokubun, and K. Hane, "A wavelength-selective add-drop switch using silicon microring resonator with a submicron-comb electrostatic actuator," Opt. Express **16**(19), 14421–14428 (2008).
8. E. Bulgan, Y. Kanamori, and K. Hane, "Submicron silicon waveguide optical switch driven by microelectromechanical actuator," Appl. Phys. Lett. **92**(10), 101110 (2008).
9. A. Liu, R. Jones, L. Liao, D. Samara-Rubio, D. Rubin, O. Cohen, R. Nicolaescu, and M. Paniccia, "A high-speed silicon optical modulator based on a metal-oxide-semiconductor capacitor," Nature **427**(6975), 615–618 (2004).
10. C. Gunn, "CMOS photonics for high-speed interconnects," IEEE Micro **26**(2), 58–66 (2006).
11. W. M. J. Green, M. J. Rooks, L. Sekaric, and Y. A. Vlasov, "Ultra-compact, low RF power, 10 Gb/s silicon Mach-Zehnder modulator," Opt. Express **15**(25), 17106–17113 (2007).
12. A. Liu, L. Liao, D. Rubin, H. Nguyen, B. Ciftcioglu, Y. Chetrit, N. Izhaky, and M. Paniccia, "High-speed optical modulation based on carrier depletion in a silicon waveguide," Opt. Express **15**(2), 660–668 (2007).
13. C. Li, L. Zhou, and A. W. Poon, "Silicon microring carrier-injection-based modulators/switches with tunable extinction ratios and OR-logic switching by using waveguide cross-coupling," Opt. Express **15**(8), 5069–5076 (2007).
14. L. Chen, K. Preston, S. Manipatruni, and M. Lipson, "Integrated GHz silicon photonic interconnect with micrometer-scale modulators and detectors," Opt. Express **17**(17), 15248–15256 (2009).
15. K. E. Moselund, P. Dainesi, M. Declercq, M. Bopp, P. Coronel, T. Skotnicki, and A. M. Ionescu, "Compact gate-all-around silicon light modulator for ultra high speed operation," Sens. Act. A **130–131**, 220–227 (2006).
16. M. R. Watts, W. A. Zortman, D. C. Trotter, G. N. Nielson, D. L. Luck, R. W. Young, "Adiabatic resonant maicrorings (ARMs) with directly integrated thermal microphotonics," CLEO Technical Digest, CPDB10 (2009).

#122083 - $15.00 USD Received 6 Jan 2010; revised 26 Feb 2010; accepted 10 Mar 2010; published 22 Mar 2010

17. H. H. Li, "Refractive index of silicon and germanium and its wavelength and temperature derivatives," J. Phys. Chem. Ref. Data **9**, 561–601 (1980).
18. T. Fukazawa, T. Hirano, F. Ohno, and T. Baba, "Low loss intersection of Si photonic wire waveguides," Jpn. J. Appl. Phys. **43**(2), 646–647 (2004).
19. K. Takahashi, E. Bulgan, Y. Kanamori, and K. Hane, "Submicron omb-drive actuators fabricated on thin single crystalline silicon layer," IEEE Trans. Ind. Electron. **56**(4), 991–995 (2009).
20. D. H. Broaddus, M. A. Foster, I. H. Agha, J. T. Robinson, M. Lipson, and A. L. Gaeta, "Silicon-waveguide-coupled high-Q chalcogenide microspheres," Opt. Express **17**(8), 5998–6003 (2009).

## 1. Introduction

Submicron silicon waveguides are promising for dense integration of optical circuits with silicon electronics in the fields of optical telecommunications and interconnects [1]. Several devices using submicron silicon waveguides were demonstrated [2–8]. In addition to a simple bent waveguide [3], functional devices such as waveguide couplers [2], filters [4–7] and optical switches [2,8], etc. were studied. The recent reports on silicon optical modulator and receiver have also attracted increasing attention to silicon photonic-electronic integration [9–15].

In the most of the important devices controlling wave-phase such as interferometric switches and filters, precise control of phase in a range over $\pi$ is essentially needed. Moreover, much larger phase-shift as multiple of $2\pi$ is also needed in several simple and complex devices such as delay-line and arrayed waveguide filter. For changing the phase of light wave in silicon waveguide, micro heater is often used on the basis of refractive index change of silicon as a function of temperature. Optical switches and wavelength filters have been demonstrated with the response time as small as 1μsec [16]. The temperature coefficient of the refractive index of silicon is $5.7\text{x}10^{-3\%}$/deg [17], which corresponds to $2\pi$ phase delay for 100μm long silicon waveguide at temperature difference of 100deg. Therefore a long waveguide at high temperature is needed for the multiple phase-shifts of $2\pi$ in addition to the large heat dissipation (~100mW) to silicon due to the relatively larger heat conductivity. In the case of the electro-optical effects of silicon, the light modulator and tunable filters have been reported [11–15]. The switching time is much faster than the thermal mechanism. However, the electro-optical coefficient is usually small, so that the power consumption by carrier injection increases for obtaining a large static phase-shift. Therefore, there are few techniques to obtain a large static phase-shift with low power consumption in a small region.

In this paper, a phase-shifter using silicon waveguide couplers with an ultra-small electro-mechanical actuator is proposed. The design and fabrication of the proposed device are presented. Applying the voltage of 31V with negligible power consumption, the phase shift of $3.0\pi$ is obtained in the device size of 50μm x 85μm.

## 2. Structure and principle

Figure 1 shows the schematic diagram of the proposed phase-shifter, which consists of input/output waveguides, movable waveguide and micro-electro-mechanical actuator. The movable waveguide includes waveguide couplers at both ends with the input and output waveguides. The movable waveguide is connected to the actuator with low optical loss suspension bridges [18] and suspended in air by the springs of the actuator. Light in the input waveguide is transmitted partially or totally through the air gap between the input waveguide and the movable waveguide by adjusting the gap and length of the coupler in coupling region. The optical arrangement of the coupler between the movable waveguide and the output waveguide is similar to that of the input coupler. The movable waveguide is translated parallel to the input/output waveguides with keeping the air gap of couplers as shown in Fig. 1. If the coupling condition is kept constant while the movable waveguide is translated, the total optical path from the input to the output can be varied by the displacement of the movable waveguide. The range of phase-shift by the waveguide displacement is dependent on the actuator displacement as well as the properties of silicon waveguide and coupler. The actuator consists of electrostatic comb and springs. The movable comb suspended by the springs is connected to the movable waveguide as shown in Fig. 1.

#122083 - $15.00 USD Received 6 Jan 2010; revised 26 Feb 2010; accepted 10 Mar 2010; published 22 Mar 2010

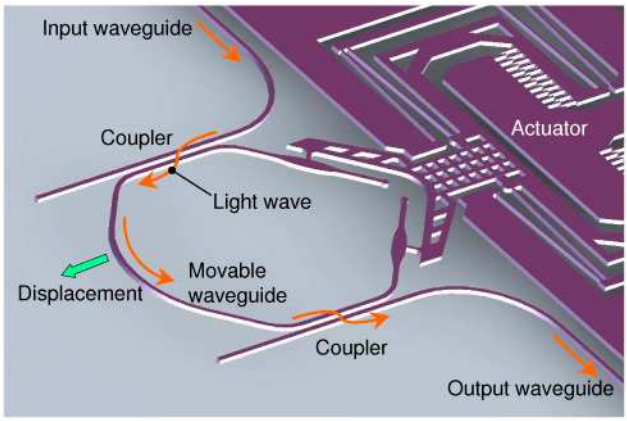


Fig. 1. Schematic diagram of submicron silicon waveguide phase-shifter with an ultra-small actuator.

In order to demonstrate the proposed phase-shifter experimentally, it is necessary to detect the phase of output wave. We design a Mach-Zehnder Interferometer (MZI) consisting of the proposed device and a fixed waveguide. The couplers are designed to have 50% separation efficiency (−3dB optical coupler). Figure 2 shows the mask-pattern of the MZI constructed from submicron silicon waveguides and the micro actuator. The size of the interferometer including actuator is 50μm wide and 85μm long. The waveguides are suspended in air, and the cross section of waveguide is 300nm wide and 260nm high, which is designed as a single mode waveguide. The air surrounding waveguides works as clad of waveguide. The MZI is separated into the two waveguides; movable waveguide and fixed waveguide. The ends of the fixed waveguide are input port and through port. The movable waveguide is connected with the actuator and can be moved in the plane of the fixed waveguide. The fixed waveguide and the movable waveguide are parallel to each other by keeping 250nm air gap with 7μm coupling length in the couplers. The movable waveguide is designed to move parallel to the fixed waveguide with the displacement of 1μm at the voltage of 30V by the actuator while keeping the air gap and the coupling length.

In the ideal case of MZI, the output intensities at through port ($I_t$) and drop port ($I_d$) are expressed by,

$$I_t = I_0 \left\{ \cos^2(2\kappa l)\cos^2\left(\frac{\phi}{2}\right) + \sin^2\left(\frac{\phi}{2}\right) \right\}, \tag{1}$$

$$I_d = I_0 \sin^2(2\kappa l)\cos^2\left(\frac{\phi}{2}\right), \tag{2}$$

$$\phi = \frac{2\pi}{\lambda}(L - 2x). \tag{3}$$

Here $I_0$ is the input light intensity, $\kappa$ is the coupling efficiency of optical coupler, $l$ denotes the coupling length of optical coupler ($\kappa l = \pi/4, 3\pi/4, 5\pi/4,..$ for −3dB coupler, here, we use $5\pi/4$), $\phi$ is the phase difference of two light waves propagating in two waveguides of MZI, $\lambda$ is the wavelength in silicon waveguide, $L$ is the initial path difference before actuating the movable waveguide. The symbol $x$ denotes the actuator displacement. The light intensities at the through and drop ports vary sinusoidally with actuator displacement. The path difference between the two waveguides decreases by the value twice larger than the actuator displacement since the two couplers are connected to the movable waveguide.

In order to evaluate the optical properties obtained from Eqs. (1) and (2), it is necessary to calculate the value of $\kappa l$ with the effective refractive index $n_{eff}$ of silicon waveguide. We used

#122083 - $15.00 USD Received 6 Jan 2010; revised 26 Feb 2010; accepted 10 Mar 2010; published 22 Mar 2010

the finite difference time domain method (FDTD, Crystal Wave) and the beam propagation method (BPM, Mode PROP) as rigorous electromagnetic theory for the structure described below. The refractive index of silicon was assumed to be 3.476.

In Fig. 2, the detailed design of the fabricated device is as follows. The movable waveguide is suspended by 1.2μm wide and 8.0μm long elliptical bridges with 0.2μm wide 1.5μm long Si suspension arms, which connect the movable waveguide to a V-shaped suspension structure of the actuator. The gap between the waveguides of the coupler is designed to be 0.25μm. The radius of the movable waveguide at the end of the coupler is 5.0μm, and the radius of the center part of the movable waveguide is 10.0μm. The movable waveguide is totally 69.4μm long between the suspension arms. The fixed waveguide is also supported by the elliptical bridges at the three points from the input port to output port. The radius of the fixed waveguide is designed to be 7.0μm. The movable and fixed waveguides are 35.6μm and 57.5μm long respectively between the ends of the two couplers under the initial condition of actuator. The lowest TM mode wave is eliminated by a TE-mode selector (not shown in Fig. 2).

The electrostatic comb-drive actuator is used to translate the movable waveguide [19]. The area of the actuator is 25μm wide and 50μm long. The comb finger is 250nm wide, 260nm thick, and 2μm long, and the gap between each finger pair is 350nm. The comb area is 2.5μm wide and 8μm long. Doubly folded springs are utilized in the microactuator. Each of the spring elements is a straight silicon bar with the width of 250nm, the thickness of 260nm and the length of 17.5μm, which corresponds to an equivalent spring constant of 0.23N/m.

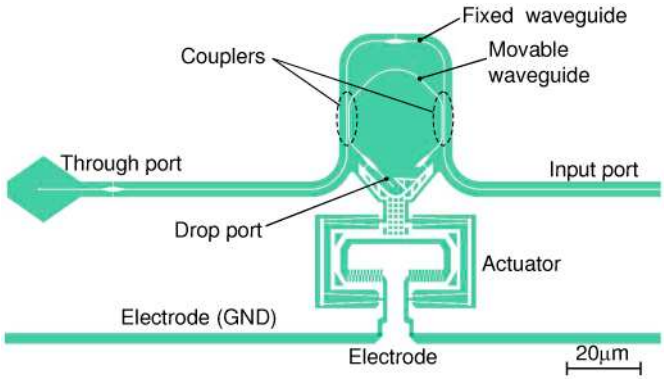


Fig. 2. Design of the Mach-Zehnder interferometer consisting of fixed waveguide, movable waveguide and actuator.

## 3. Fabrication and experiments

In the fabrication of the proposed device, a SOI wafer with 260nm thick top silicon layer and 2μm thick buried oxide layer on 625μm thick silicon substrate was used. First, 350nm thick positive resist polymer (ZEON ZEP-520A) was coated on the SOI wafer, and it was exposed by using an electron-beam patterning machine (JEOL JBX-5000LS). After developing the resist polymer, the top silicon layer was etched by fast atom beam (FAB) (Ebara FAB-60ML). The FAB consisted of neutral molecular fragments extracted from a dc $SF_6$ gas plasma. The resist polymer was removed by $O_2$ plasma ashing after FAB etching. After the lithographic processes, the SOI wafer was cleaved to obtain a facet of input waveguide for coupling light. Finally, the $SiO_2$ layer was etched by hydrofluoric acid vapor to obtain the freestanding structure of MZI.

In the measurement of the fabricated MZI, a tunable infrared laser (Agilent 81682A) was used as light source at the wavelength around 1.5μm. For coupling the laser light to the end surface of the input port of MZI, a lensed single mode fiber was used. The light intensities at the through port and the drop port were measured from the spot images of scattered light at the ends of waveguides using an IR camera (Goodrich SU320KTS-1.7RT). The gamma value

#122083 - $15.00 USD Received 6 Jan 2010; revised 26 Feb 2010; accepted 10 Mar 2010; published 22 Mar 2010

of the IR camera was calibrated to be 1.0, and the uniformity of the camera image was better than 1% in the intensity evaluation. The ends of the waveguides were rounded to measure the scattered light efficiently. Although the emissions from the rounded ends of the waveguides were directional, the detection efficiencies normal to the substrate were equal for the respective output ports because of the symmetry of the optical arrangement.

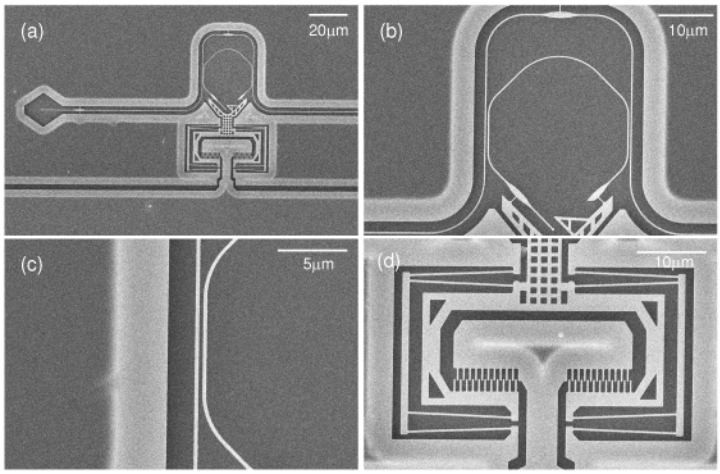


Fig. 3. Electron micrographs of the fabricated device, (a) whole view of the device, (b) movable and input/output waveguides with couplers, (c) 3dB coupler, (d) actuator.

## 4. Results and discussion

Figure 3(a) shows an electron micrograph of the whole view of the fabricated MZI. The interferometer waveguides and the actuator are well fabricated. The $SiO_2$ layer is etched about 4μm inside from the edge of top Si layer, and it is seen in pale color in Fig. 3(a). Figure 3(b) shows the magnified image of the MZI with the two waveguide couplers. The movable waveguide is connected to the actuator by the elliptical bridges to minimize the influence of the suspension arm to light wave. The one end of the movable waveguide is terminated by a small rounded end, which is used for scattering the light dropped from the second coupler. The second coupler is magnified in Fig. 3(c). The waveguides of the coupler are 245nm wide, smoothly formed and aligned parallel with each other with the air gap of about 0.28μm, which agrees well with the designed value. The surfaces of the parallel waveguides are seen smooth with the roughness less than 15nm. The radius of the movable waveguide at the end of the coupler also agrees well with the designed value of 5.0μm. Figure 3(d) shows the image of the actuator. The actuator is also fabricated well with the 20 finger pairs. The spring width of the actuator is measured to be about 0.27μm.

The laser light at the wavelength of 1.459μm was used as incident light for the input waveguide of the fabricated MZI, and the IR image of the output ports was obtained from the top of the device. Changing the voltage applied to the actuator, the intensities of the light spots generated by the scatted light from the ends of the output waveguides varied periodically with the displacement of the movable waveguide. Figure 4(a) shows the IR image obtained at the voltage of 15V. The maximum intensity at the through port is observed and the light spot intensity at the drop port is minimum. When the voltage is increased to 25V, the intensity at the through port becomes minimum and that at the drop port becomes maximum as shown in Fig. 4(b).

#122083 - $15.00 USD Received 6 Jan 2010; revised 26 Feb 2010; accepted 10 Mar 2010; published 22 Mar 2010

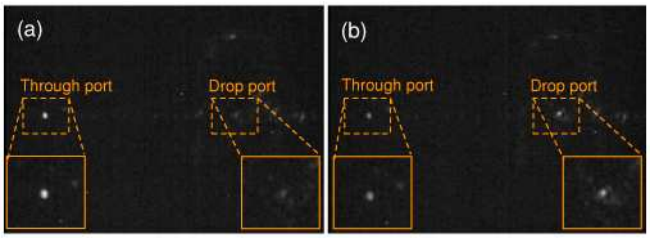


Fig. 4. Infrared camera images, (a) maximum intensity at through port at the voltage of 15V, (b) maximum intensity at drop port at 25V.

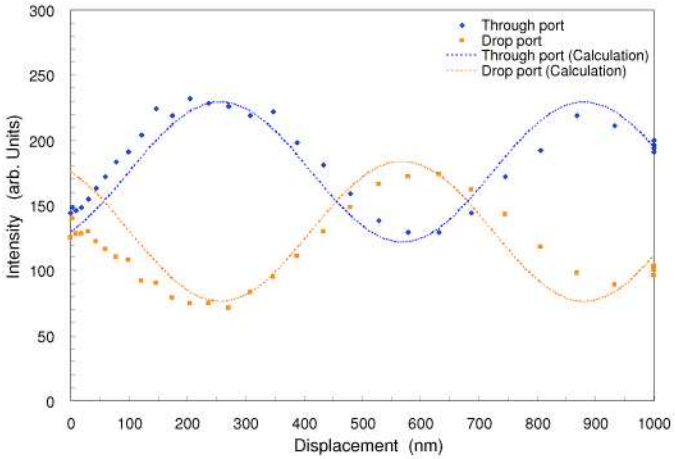


Fig. 5. Light intensities measured as a function of actuator displacement.

Figure 5 shows the light intensities measured as a function of the displacement of actuator. The intensity at the drop port as a function of the displacement is phase-shifted by 180 deg. comparing with that at the through port. It is considered that the offset intensity of the outputs of the MZI is caused by stray light from the light source since the minimum intensity at drop port is always theoretically zero. The light intensity varies periodically with the period of about 670nm. This corresponds to the low equivalent refractive index of silicon waveguide under our experimental conditions [20]. The theoretical calculations using Eqs. (1) and (2) and the values of $\kappa\, l$ and $n_{eff}$ obtained form FDTD are also shown in Fig. 5 after adding the offset intensity. From the measured phase-shift of $3.0\pi$ at the displacement of 1μm, the effective refractive index $n_{eff}$ was obtained to be 1.1. On the other hand, the value of $n_{eff}$ calculated by BPM was equal to 1.17, which agreed with the measured value. Fitting Eqs. (1) and (2) to the measured intensities at the through and drop ports after subtracting the offset intensity at the drop port, the coupling coefficient $\kappa\, l$ was obtained to be $1.36\pi$. On the other hand,, the value of $\kappa\, l$ was calculated to be $1.34\pi$ by FDTD for the fabricated structure. Although those values of $\kappa\, l$ were slightly deviated from the initial design for −3dB coupler with $\kappa\, l=5\pi/4$, the measured output intensities as a function of displacement were explained by the theoretical calculation based on FDTD.

The insertion loss of the fabricated device was roughly estimated to be −1dB from the intensity of scattered light in the IR image. The waveguide loss of the fabricated straight waveguide was about −10dB/cm. Therefore the different losses at different arms of the MZI were caused mainly by the loss of the elliptical bridge of the fixed waveguide. The loss of the elliptical bridge was around −0.1dB, and thus, from the theoretical calculation, the different losses at different arms generated a decrease of the modulation contrast by about −0.1dB.

With the maximum displacement of 1.0μm at the voltage of 31V, the phase shift of $3.0\pi$ is obtained. The increase of the displacement of actuator can further increase the range of phase-

#122083 - $15.00 USD Received 6 Jan 2010; revised 26 Feb 2010; accepted 10 Mar 2010; published 22 Mar 2010

shift. The response time of the phase shifter is limited by the first resonant frequency of the actuator. Since the resonant frequency of the actuator is measured to be about 153kHz, the response time is considered to be roughly 10μsec. Due to the capacitive operation of the electrostatic comb-drive actuator, the power consumption is negligible compared with the case using the thermal index variation of silicon waveguide.

## 5. Conclusion

A phase-shifter using the movable waveguide and couplers was proposed and fabricated by silicon micro machining. The movable waveguide and couplers were connected to an ultra-small electrostatic comb-drive actuator. Composing a MZI using the proposed device, the phase-shift of 3.0π was obtained at the actuator displacement of 1.0μm and the voltage of 31V. Since the device size is as small as 50μm x 85μm and the power consumption is negligible, the proposed phase-shifter can be integrated efficiently in silicon waveguide circuits and will be valuable for several optical devices such as switch and delay-line.

## Acknowledgements

This work was partially supported by Grant-in-Aid for Scientific Research and JST (FICFAT).

#122083 - $15.00 USD Received 6 Jan 2010; revised 26 Feb 2010; accepted 10 Mar 2010; published 22 Mar 2010